UNCECOMP 2015
1st ECCOMAS Thematic Conference on
International Conference on Uncertainty Quantification in
Computational Sciences and Engineering
M. Papadrakakis, V. Papadopoulos, G. Stefanou (eds.)
Crete Island, Greece, 25–27 May 2015

NEW CONTINUOUS CONTROL METHODOLOGY FOR NONLINEAR DYNAMICAL SYSTEMS WITH UNCERTAIN PARAMETERS

Hancheol Cho[1], Thanapat Wanichanon[2], and Firdaus E. Udwadia[3]

[1] Samsung Techwin Co., Ltd.
Power Systems Division
701 Sampyeong-dong, Bundang-gu, Seongnam-si, Gyeonggi-do 463-400, Republic of Korea
e-mail: hancheol.cho@gmail.com

[2] Mahidol University
Department of Mechanical Engineering
25/25 Puttamonthon, Nakorn Pathom 73170, Thailand
e-mail: thanapat.wan@mahidol.ac.th

[3] University of Southern California
Department of Aerospace and Mechanical Engineering
3650 McClintock Ave. OHE 430K, Los Angeles, CA 90089, United States of America
e-mail: fudwadia@usc.edu

Keywords: Nonlinear Dynamical Systems, Fundamental Equation of Constrained Motion, Sliding Mode Control, PID Control, Lyapunov Stability.

Abstract. *This paper presents a new reference-tracking control methodology for nonlinear dynamical systems in the presence of unknown, but bounded, uncertainties in the system. To this end, two controllers are combined. A nonlinear controller is first developed to exactly track the desired reference trajectory assuming no uncertainties in the nonlinear nominal system. The entire nonlinear dynamics of the nominal system is included and no approximations/linearizations are made. Next, an additional continuous controller is developed in closed form to compensate for uncertainties in the physical model by generalizing the concept of sliding surfaces. Unlike conventional sliding mode control, this Lyapunov-based approach eliminates the chattering problem by replacing a signum function with a set of continuous functions that may have different forms depending on practical considerations related to actuator implementation. Among these possible forms, special attention is paid to a controller with a PID form. By using Lyapunov stability theory it is shown that this additional controller forces the tracking errors that arise because of the uncertainties in the system to move into a small, user-specified region around the generalized sliding surface. Once these tracking errors enter this small region, if the original nonlinear system is assumed to be linearizable, then linear control theory will ensure that they will further converge to even smaller values. A numerical example is provided, in which a satellite in the presence of air drag is required to maintain a specific, circular orbit around the Earth whose gravity field is imprecisely known.*

The example demonstrates the accuracy, efficiency, and ease of implementation of the control methodology.

1 INTRODUCTION

The reference-tracking problem arises in many practical situations such as the steering control of an automobile and the flight control of a missile. Applications to astronautical engineering include orbital station-keeping of a satellite and formation-keeping of multiple satellites. In this field, optimal control is especially critical in that the number of thruster burns a satellite can implement during its lifetime is limited.

If a linear equation of motion for a dynamical system is utilized, the optimal solution may be easily found by solving the LQR (Linear Quadratic Regulator) problem [1]. However, if the system is nonlinear so that linear control theory cannot apply, the tracking problem becomes challenging and it is much more difficult to find analytical solutions. In the field of analytical dynamics, recently a new, analytical approach [2,3] has been proposed that obtains the equation of motion for constrained systems, which is sometimes called the *fundamental equation of constrained motion (FECM)*, whether the constraints are holonomic or nonholonomic. One can recast the given trajectory requirements on a dynamical system as constraints on it so that the constraint force now becomes the control force that is required to make the dynamics satisfy the trajectory requirements (constraints) placed on it. This methodology not only carries all the nonlinearities inherited from the original dynamical system, but also expresses the control forces succinctly in closed form [3,4], which inspires many applications. For example, formation-keeping control schemes for a set of satellites were proposed where the reference trajectory is Keplerian [5] or arbitrary [6]. Also, a rigorous, analytical analysis for the orbital and attitude control algorithms of satellites in a formation was performed, deepening insight into the satellite formation system with orbital and attitude requirements [7]. Also, this resultant constraint force is optimal in the sense that it minimizes the control cost *at each instant of time*.

However, this strategy is said to be ideal because it is based on the assumption that the dynamical model is perfectly known and the states are precisely measured. In real-life dynamical systems, exact modeling is never possible because there always exist parameter uncertainties and disturbances, making our knowledge of the dynamical system *uncertain*. Sliding mode control (SMC) is widely adopted to cope with such uncertainties due to its simplicity and robustness [8,9]. However, it generally induces a serious problem called chattering, which involves high control oscillations and sometimes brings unintended nonlinearities into the system. The two common methods to avoid the chattering problem are the boundary layer approach [10,11] and the use of high-order SMC [12]. In the boundary approach, however, less chattering occurs at the expense of worse control performance (i.e., larger tracking errors). Also, the use of high-order SMC usually requires complex calculations.

To obviate these difficulties, in this paper the tracking control problem is solved using a two-step approach. In the first step, a nonlinear controller is analytically developed using the concept of the FECM. All the nonlinearities of the original system are preserved and no approximations are made. In this step, the system is assumed to be 'nominal' in the sense that it is our best assessment of the actual system that can be obtained through measurements and/or modeling; accordingly no uncertainties are considered. The discrepancies caused by ignoring the uncertainties are compensated by using an additional controller and this comprises the second step of our approach. This controller is in a sense a generalization of the boundary layer approach since the concept of the boundary layer is employed to prove the Lyapunov stability. However, the new SMC developed herein has more variant forms for pragmatic implementation and more flexibility in choosing control gains to acquire better control performance.

Among others, a special PID-form of SMC is analyzed in detail due to its simplicity and advantages, thanks to linear control theory. In other words, much better performance is guaranteed, i.e., very small steady-state errors, less chattering, and faster response, thus extending the previous approach presented in Ref. [13] in which the tracking accuracy is not improved within the boundary layer. As a numerical example an orbital station-keeping control problem is provided in which a satellite in the presence of atmospheric drag is orbiting the Earth while the non-uniform gravitational field that it is subjected to is imprecisely known. This simulation confirms the validity and reliability of the novel control approach proposed in this paper.

2 EXACT REFERENCE-TRACKING CONTROL FOR NONLINEAR NOMINAL SYSTEMS WITH NO UNCERTAINTIES

In this paper, two different controllers will be combined to track the desired reference trajectory in the presence of system uncertainties. In this section, the first controller will be developed assuming *no uncertainties* in the nonlinear nominal system – our best assessment of the actual physical system. Without any constraints, the equation of motion of a dynamical system is described by the Lagrange's equation:

$$M(q,t)\ddot{q}(t)=Q\left[q(t),\dot{q}(t),t\right], \tag{1}$$

or

$$\ddot{q}(t)=M^{-1}(q,t)Q\left[q(t),\dot{q}(t),t\right]:=a(t), \tag{2}$$

where t represents time, $q(t)=\left[q_1(t) \quad q_2(t) \quad \cdots \quad q_n(t)\right]^T$ is a generalized displacement vector, $M>0$ is an n by n mass matrix, Q is the n by 1 given generalized force vector, and $a(t)$ is the n by 1 unconstrained acceleration vector. In addition, the superscript "T" denotes the transpose of a vector or a matrix and n is the number of the generalized coordinates.

Now it is assumed that the unconstrained system described by Eqs. (1) or (2) is subjected to p constraints which are of the form

$$\varphi_j(q,\dot{q},t)=0,\ j=1,2,\cdots,p. \tag{3}$$

Differentiating Eq. (3) with respect to time once (for nonholonomic constraints) or twice (for holonomic constraints) yields the following constraint equation:

$$A\left[q(t),\dot{q}(t),t\right]\ddot{q}(t)=b\left[q(t),\dot{q}(t),t\right], \tag{4}$$

where the matrix A is a p by n matrix and b is a p by 1 vector.

Then, the aim is to obtain a vector $\ddot{q}$ *in closed form* that satisfies the constraint equation, Eq. (4), and that simultaneously minimizes the required additional control effort. First, the solution to Eq. (4) is explicitly given by [14]:

$$\ddot{q}=A^{\dagger}b+\left(I-A^{\dagger}A\right)h, \tag{5}$$

where I is the n by n identity matrix, the superscript "†" denotes the Moore-Penrose generalized inverse, and h is an arbitrary n by 1 vector. From the perspective of controller design, it is generally desired to obtain this arbitrary h so that it minimizes the following cost function at each instant of time:

$$J=(\ddot{q}-a)^T M(\ddot{q}-a). \tag{6}$$

Substituting h that minimizes Eq. (6) back to Eq. (5), we finally obtain the following equation of motion in the presence of the constraints given by Eq. (3) [14]:

$$\ddot{q}(t) = a + M^{-1}A^T\left(AM^{-1}A^T\right)^{\dagger}(b - Aa). \tag{7}$$

From Eq. (7), the required control force $Q^c(t)$ is easily obtained in closed form:

$$Q^c(t) := M(\ddot{q} - a) = A^T\left(AM^{-1}A^T\right)^{\dagger}(b - Aa). \tag{8}$$

Originally, this idea is inspired by a recent finding in analytical dynamics [2-4] and Eq. (7) is called the *fundamental equation of constrained motion* (FECM). It must be noted that we have explicitly obtained the control force, Eq. (8), while preserving the full nonlinearities of the original dynamical system. In what follows we shall interpret the constraints given in Eq. (3) as the trajectory requirements that the dynamical system described in Eq. (1) is required to track [3,4].

Up to now, the exact control force $Q^c(t)$ has been developed assuming no uncertainties in the dynamical system. In the next section a new additional controller will be derived and added in order to handle the effects of uncertainties.

3 CONTINUOUS SLIDING MODE CONTROL TO COPE WITH SYSTEM UNCERTAINTIES

The controller developed based on the FECM in the previous section requires the *exact* information about the generalized displacement and velocity in real time. However, this is not the case in the actual physical world because of the imprecise modeling, measurement errors, and so on. Hence, a controller used in the real world is required to be robust in the sense that it can successfully track the reference trajectory regardless of these uncertainty effects. A sliding mode control is generally adopted to cope with uncertainties due to its simplicity and high robustness. However, one main drawback of the conventional sliding mode control is the chattering problem: high-frequency oscillations in the states and/or in the control forces. Generally, a boundary layer approach is employed to avoid this problem, which uses the saturation function in place of the discontinuous signum function, but this method results in a tradeoff between the chattering and tracking errors, so the errors may not converge although they are bounded. In the present paper, it will be shown that instead of the existing signum or saturation functions, many other continuous functions are possible to be used to avoid the chattering phenomenon.

For the constrained nominal system with no uncertainties, the equation of motion is given by

$$M\ddot{q}(t) = Q(q, \dot{q}, t) + Q^c(t), \tag{9}$$

where $Q(q, \dot{q}, t)$ is a given generalized force and $Q^c(t)$ is the generalized control force that is explicitly given in Eq. (8). This generalized control force is added to exactly satisfy the given trajectory requirements (constraints) given in Eq. (3). However, in the real world, it may not possible to exactly determine the mass matrix M and the given force Q. Hence, application of the control force $Q^c(t)$ to the actual (unknown) system generally results in

$$M_a\ddot{q}(t) \neq Q_a(q, \dot{q}, t) + Q^c(t), \tag{10}$$

where M_a and Q_a are the actual (unknown) mass matrix and the actual (unknown) given force, respectively. In general, the left hand side in relation (10) does not equal the right hand side because $Q^c(t)$ does not exactly compensate the difference between $M_a\ddot{q}$ and Q_a due to uncertainties in the actual system. Hence, it is necessary to apply an additional generalized control force $Q^u(t)$ to equate both sides in Eq. (10). Thus, to successfully track the given reference trajectory even in the presence of system uncertainties the equation of motion becomes

$$M_a\ddot{q}_c(t) = Q_a(q_c, \dot{q}_c, t) + Q^c(t) + Q^u(t), \tag{11}$$

where $q_c(t)$ denotes the controlled, actual generalized displacement vector. The additional control force $Q^u(t)$ will be developed by generalizing the concept of sliding mode control. From here on for brevity, the arguments of the various quantities will be suppressed unless required for clarity.

First, from Eqs. (9) and (11), we have

$$\ddot{q} = M^{-1}(Q + Q^c), \tag{12a}$$

$$\ddot{q}_c = M_a^{-1}(Q_a + Q^c + Q^u). \tag{12b}$$

If the error $e(t)$ is defined by

$$e(t) = q_c - q, \tag{13}$$

the differentiation of e with respect to time twice yields

$$\begin{aligned} \ddot{e} &= \ddot{q}_c - \ddot{q} \\ &= M_a^{-1}(Q_a + Q^c + Q^u) - M^{-1}(Q + Q^c) \\ &= \left[M_a^{-1}(Q_a + Q^c) - M^{-1}(Q + Q^c)\right] + M_a^{-1}Q^u. \end{aligned} \tag{14}$$

If the following is defined,

$$\begin{aligned} \delta\ddot{q} &\equiv M_a^{-1}(Q_a + Q^c) - M^{-1}(Q + Q^c), \\ u &\equiv M_a^{-1}Q^u, \end{aligned} \tag{15}$$

Eq. (14) can be rewritten as

$$\ddot{e} = \delta\ddot{q} + u. \tag{16}$$

Here, it is assumed that the value of $\delta\ddot{q}$ is uncertain, but it is bounded by

$$\|\delta\ddot{q}\|_\infty \le \Gamma, \tag{17}$$

where Γ is a positive constant and $\|\cdot\|_\infty$ denotes an infinity-norm of a vector.

Then, let us consider the generalized sliding surface s defined by

$$s \equiv \dot{e} + be + k\int e\,dt \quad (b > 0, k \ge 0), \tag{18}$$

where b and k are constants, and $s = \begin{bmatrix} s_1 & s_2 & \cdots & s_n \end{bmatrix}^T$. From Eq. (18), we have

$$s_i = \dot{e}_i + be_i + k\int e_i\,dt \quad (i = 1, 2, \cdots, n). \tag{19}$$

It is not difficult to show that if $s_i = 0$, then e_i converges to zero asymptotically as $t \to \infty$.

Now, let us define the Lyapunov function V by:

$$V = \frac{1}{2}s^T s = \frac{1}{2}\sum_{i=1}^{n} s_i^2. \tag{20}$$

Its derivative is given by

$$\dot{V} = s^T \dot{s} = \sum_{i=1}^{n} s_i \dot{s}_i = \sum_{i=1}^{n} s_i \left(\ddot{e}_i + b\dot{e}_i + ke_i\right) = \sum_{i=1}^{n} s_i \left(\delta\ddot{q}_i + u_i + b\dot{e}_i + ke_i\right). \tag{21}$$

Then, the aim is to find an additional control force u_i so that $\dot{V}$ is negative. The conventional sliding mode controller utilizes the following control force u_i:

$$u_i = -b\dot{e}_i - ke_i - \Gamma \operatorname{sgn}\left(s_i\right), \tag{22}$$

because then Eq. (21) becomes

$$\dot{V} = \sum_{i=1}^{n} s_i \left(\delta\ddot{q}_i + u_i + b\dot{e}_i + ke_i\right) = \sum_{i=1}^{n} s_i \left[\delta\ddot{q}_i - \Gamma \operatorname{sgn}\left(s_i\right)\right], \tag{23}$$

and $\dot{V} < 0$ always holds. However, the discontinuity of $\operatorname{sgn}(\cdot)$ function generally results in the undesirable chattering problem.

In order to avert chattering, let us first consider a region where $|s_i| > \varepsilon$ holds ($\varepsilon > 0$ is a small positive number), then the following inequality is satisfied:

$$s_i \delta\ddot{q}_i < \frac{\Gamma}{\varepsilon} s_i^2. \tag{24}$$

Proof: If s_i and $\delta\ddot{q}_i$ have opposite signs, then Eq. (24) always holds because the right hand side is always positive. Hence, let us consider the following two cases when s_i and $\delta\ddot{q}_i$ have the same sign.

Case 1. When $s_i > 0$ and $0 \le \delta\ddot{q}_i \le \Gamma$,

since $s_i > 0$, we have

$$\frac{s_i}{\varepsilon} > 1 \tag{25}$$

from the assumption of $|s_i| > \varepsilon$. Multiplying both sides by $\Gamma s_i \ (>0)$ yields

$$\Gamma s_i < \frac{\Gamma}{\varepsilon} s_i^2. \tag{26}$$

From the assumption that $s_i > 0$ and $\delta\ddot{q}_i \le \Gamma$, we have

$$s_i \delta\ddot{q}_i \le \Gamma s_i, \tag{27}$$

and it follows that $s_i \delta\ddot{q}_i < \frac{\Gamma}{\varepsilon} s_i^2$.

Case 2. When $s_i < 0$ and $-\Gamma \le \delta\ddot{q}_i < 0$,

since $s_i < 0$, $|s_i| = -s_i$ and again from $|s_i| > \varepsilon$, we have

$$-\frac{s_i}{\varepsilon} > 1. \tag{28}$$

Multiplying both sides by $-\Gamma s_i \ (>0)$ yields

$$-\Gamma s_i < \frac{\Gamma}{\varepsilon} s_i^2. \tag{29}$$

From the assumption that $s_i < 0$ and $-\Gamma \le \delta \ddot{q}_i$, we have

$$s_i \delta \ddot{q}_i \le -\Gamma s_i, \tag{30}$$

and it follows that $s_i \delta \ddot{q}_i < \frac{\Gamma}{\varepsilon} s_i^2$. ❑

Then, using relation (24), Eq. (21) becomes

$$\dot{V} = \sum_{i=1}^{n} s_i \left(\delta \ddot{q}_i + u_i + b\dot{e}_i + ke_i \right) < \sum_{i=1}^{n} \left[\frac{\Gamma}{\varepsilon} s_i^2 + s_i \left(u_i + b\dot{e}_i + ke_i \right) \right]. \tag{31}$$

Let us choose the additional acceleration u_i as

$$u_i = -b\dot{e}_i - ke_i - \frac{\Gamma}{\varepsilon} s_i - f\left(s_i\right), \tag{32}$$

where $f\left(s_i\right)$ is a function to be determined. Then, Eq. (31) becomes

$$\dot{V} < \sum_{i=1}^{n} \left[\frac{\Gamma}{\varepsilon} s_i^2 + s_i \left(u_i + b\dot{e}_i + ke_i \right) \right] = \sum_{i=1}^{n} \left[-s_i f\left(s_i\right) \right]. \tag{33}$$

In brief, in the region $|s_i| > \varepsilon$, $\dot{V} < 0$ is guaranteed just if $f\left(s_i\right) = 0$ or s_i and $f\left(s_i\right)$ have the same sign. Conventionally the discontinuous signum function is used for $f\left(s_i\right)$ as noted in Eq. (22), resulting in the chattering problem, but now one can find a number of the continuous functions $f\left(s_i\right)$ that effectively avert the chattering problem.

Selection of the function $f\left(s_i\right)$ will depend on the practical control cost to be minimized or on the control performance associated with mission goals. In this paper special attention is paid to the case where

$$f\left(s_i\right) = \eta s_i, \ \left(\eta \ge 0\right) \tag{34}$$

so that s_i and $f\left(s_i\right)$ have the same sign and $\dot{V} < 0$ is guaranteed. Then the control law, Eq. (32), is nothing but a conventional PID controller with the gains $G_P = -\left(k + \frac{\Gamma b}{\varepsilon} + \eta b \right)$, $G_I = -k\left(\frac{\Gamma}{\varepsilon} + \eta \right)$, and $G_D = -\left(b + \frac{\Gamma}{\varepsilon} + \eta \right)$. In brief, the control law $u_i\left(t\right)$ is given by:

$$\begin{aligned} u_i\left(t\right) &= -b\dot{e}_i - ke_i - \frac{\Gamma}{\varepsilon} s_i - \eta s_i \\ &= -\left(k + \frac{\Gamma b}{\varepsilon} + \eta b \right) e_i - k\left(\frac{\Gamma}{\varepsilon} + \eta \right) \int e_i dt - \left(b + \frac{\Gamma}{\varepsilon} + \eta \right) \dot{e}_i \\ &= G_P e_i + G_I \int e_i dt + G_D \dot{e}_i, \end{aligned} \tag{35}$$

where $k \geq 0$, $b > 0$, $\varepsilon > 0$, $\Gamma > 0$, and $\eta \geq 0$.

Up to now, it has been shown that in the region $|s_i| > \varepsilon$, $\dot{V} < 0$ is guaranteed if the control law, Eq. (32), is used where $f(s_i) = 0$ or s_i and $f(s_i)$ have the same sign. On the contrary, if $|s_i| \leq \varepsilon$, $\dot{V} < 0$ is not guaranteed and the errors may not converge to zero (although they are bounded). This is because the control $u_i(t)$ forces the states into the region bounded by $|s_i| = \varepsilon$ instead of onto the sliding surface $s_i = 0$. However, if ε is small enough, the errors will be also small enough so that the original nonlinear system can be *linearized*. Then, by linear control theory, the PID controller, Eq. (35), can force the errors to go to much smaller values with proper gain tuning. In brief, the use of the PID controller given by Eq. (35) forces the states into the region bounded by $|s_i| = \varepsilon$, and once the states enter this region we know from linear control theory that the errors will converge to very small values. Thus by taking advantage of both linear and nonlinear control theory improved performance is obtained with no chattering and with faster response, in the sense that gain-tuning is simplified and robustness is guaranteed.

4 NUMERICAL EXAMPLE

In this section a numerical example is given to validate the control methodology developed in the previous sections. The numerical integration throughout this paper is done in the Matlab/Simulink environment, using a fixed time step of 0.01 second using the ode4 Runge-Kutta integrator.

First, we consider a nominal system (with no uncertainty) in which a satellite is orbiting the spherical Earth *under atmospheric drag*. The equation of motion of the satellite without any constraint on its motion is given by [15]

$$a(t) = -\frac{GM_{\oplus}}{\left(X^2+Y^2+Z^2\right)^{3/2}}\begin{bmatrix} X \\ Y \\ Z \end{bmatrix} - \frac{1}{2}C_D\frac{S_{ref}}{m}\rho_0\|v\|\begin{bmatrix} \dot{X} \\ \dot{Y} \\ \dot{Z} \end{bmatrix}, \quad (36)$$

where G is the universal gravitational constant, $M_{\oplus}$ is the mass of the Earth, and $\begin{bmatrix} X & Y & Z \end{bmatrix}^T$ is the position vector in the ECI (Earth-Centered Inertial) frame. Here C_D is the drag coefficient, S_{ref} is the cross-sectional area of the satellite, m is the mass of the satellite, ρ_0 is the atmospheric density of the Earth, $v = \begin{bmatrix} \dot{X} & \dot{Y} & \dot{Z} \end{bmatrix}^T$ is the velocity vector of the satellite in the ECI frame, and $\|v\|$ is the Euclidean norm of v. In the numerical example, $C_D = 0.47$, $S_{ref} = \pi \ (\mathrm{m}^2)$, $m = 100 \ (\mathrm{kg})$, and $\rho_0 = 1.0 \times 10^{-11} \ (\mathrm{kg/m}^3)$ are assumed.

The satellite is constrained to remain in a nominal circular orbit with a radius of $r_0 = 7.0 \times 10^6$ m, $i = 80^\circ$, $\Omega = 30^\circ$, $\omega = 0^\circ$, where i, Ω, and ω are the inclination, the longitude of the ascending node, and the argument of perigee of the satellite, respectively, with the mean motion of $n = \sqrt{\frac{GM_{\oplus}}{r_0^3}} = 1.078 \times 10^{-3}$ (rad/s). This constraint can be represented in the Perifocal Frame [15] as

$$x^2 + y^2 = r_0^2,\ z = 0, \tag{37}$$

where $\begin{bmatrix} x & y & z \end{bmatrix}^T$ is the position vector of the satellite in the Perifocal Frame. The conversion between the Perifocal Frame and the ECI frame is given by [5]

$$\begin{bmatrix} x \\ y \\ z \end{bmatrix} = R \begin{bmatrix} X \\ Y \\ Z \end{bmatrix}, \tag{38}$$

where the transformation matrix R, which is constant, is given by

$$R = \begin{bmatrix} R_{11} & R_{12} & R_{13} \\ R_{21} & R_{22} & R_{23} \\ R_{31} & R_{32} & R_{33} \end{bmatrix} = \begin{bmatrix} \cos\Omega\cos\omega - \sin\Omega\cos i\sin\omega & \sin\Omega\cos\omega + \cos\Omega\cos i\sin\omega & \sin i\sin\omega \\ -\cos\Omega\sin\omega - \sin\Omega\cos i\cos\omega & \cos\Omega\cos i\cos\omega - \sin\Omega\sin\omega & \sin i\cos\omega \\ \sin\Omega\sin i & -\cos\Omega\sin i & \cos i \end{bmatrix}. \tag{39}$$

Then, the trajectory constraint equation, Eq. (37), is now represented in the ECI frame as

$$\begin{gathered} \left(R_{11}^2 + R_{21}^2\right)X^2 + \left(R_{12}^2 + R_{22}^2\right)Y^2 + \left(R_{13}^2 + R_{23}^2\right)Z^2 \\ +2\left(R_{11}R_{12} + R_{21}R_{22}\right)XY + 2\left(R_{12}R_{13} + R_{22}R_{23}\right)YZ + 2\left(R_{13}R_{11} + R_{23}R_{21}\right)ZX = r_0^2, \\ R_{31}X + R_{32}Y + R_{33}Z = 0. \end{gathered} \tag{40}$$

Differentiating Eq. (40) with respect to time twice to get the form of Eq. (4) yields

$$\begin{gathered} \begin{bmatrix} \left(R_{11}^2 + R_{21}^2\right)X + \left(R_{11}R_{12} + R_{21}R_{22}\right)Y + \left(R_{13}R_{11} + R_{23}R_{21}\right)Z & \left(R_{12}^2 + R_{22}^2\right)Y + \left(R_{11}R_{12} + R_{21}R_{22}\right)X + \left(R_{12}R_{13} + R_{22}R_{23}\right)Z & \left(R_{13}^2 + R_{23}^2\right)Z + \left(R_{12}R_{13} + R_{22}R_{23}\right)Y + \left(R_{13}R_{11} + R_{23}R_{21}\right)X \\ R_{31} & R_{32} & R_{33} \end{bmatrix} \begin{bmatrix} \ddot{X} \\ \ddot{Y} \\ \ddot{Z} \end{bmatrix} \\ = -\begin{bmatrix} \left(R_{11}^2 + R_{21}^2\right)\dot{X}^2 + \left(R_{12}^2 + R_{22}^2\right)\dot{Y}^2 + \left(R_{13}^2 + R_{23}^2\right)\dot{Z}^2 + 2\left(R_{11}R_{12} + R_{21}R_{22}\right)\dot{X}\dot{Y} + 2\left(R_{12}R_{13} + R_{22}R_{23}\right)\dot{Y}\dot{Z} + 2\left(R_{13}R_{11} + R_{23}R_{21}\right)\dot{Z}\dot{X} \\ 0 \end{bmatrix}. \end{gathered} \tag{41}$$

The required nominal control force, $Q^c(t)$, to exactly track this circular orbit is then given by the FECM as described in Eq. (8). The initial conditions in the ECI frame used for the simulation also satisfy the constraints Eq. (40), which are chosen as follows:

Table 1 Initial conditions in the ECI frame

X_0 (m)	6.0628e+6
Y_0 (m)	3.5e+6
Z_0 (m)	0
$\dot{X}_0$ (m/s)	-6.5518e+02
$\dot{Y}_0$ (m/s)	1.1348e+03
$\dot{Z}_0$ (m/s)	7.4314e+03

Figure 1 shows the controlled trajectory in the Perifocal Frame and the constraints Eq. (37) are quite well satisfied. The duration of time used for numerical integration is chosen as one orbital period.

As yet there is no uncertainty in the system. This system wherein there are no uncertainties is referred to as the nominal system. Now the Earth's gravitational field, which was assumed to be uniform for the nominal system, is actually not so. It is assumed that the gravitational field causes the acceleration of the satellite to be perturbed, with the perturbation given by

$$\delta\ddot{q}(t) = \begin{bmatrix} \cos\Omega_{\oplus}t & -\sin\Omega_{\oplus}t & 0 \\ \sin\Omega_{\oplus}t & \cos\Omega_{\oplus}t & 0 \\ 0 & 0 & 1 \end{bmatrix} \sum_{n=2}^{\infty}\sum_{m=0}^{n} g_{n,m}, \tag{42}$$

where $\Omega_{\oplus}$ is the mean rotation rate of the Earth and $g_{n,m}$ is given by [16]

$$g_{n,m} = \frac{GM_{\oplus}R_{\oplus}^{n}}{r_{ITRF}^{n+m+1}} \begin{bmatrix} \dfrac{C_{n,m}\Gamma_{m} + S_{n,m}\Pi_{m}}{r_{ITRF}} \left\{ P_{n,m+1}\hat{Z}_{ITRF} - \left(S_{\lambda}P_{n,m+1} + (n+m+1)P_{n,m} \right)\hat{r}_{ITRF} \right\} \\ +mP_{n,m}\left\{ \left(C_{n,m}\Gamma_{m-1} + S_{n,m}\Pi_{m-1} \right)\hat{X}_{ITRF} + \left(S_{n,m}\Gamma_{m-1} - C_{n,m}\Pi_{m-1} \right)\hat{Y}_{ITRF} \right\} \end{bmatrix}. \tag{43}$$

Here, $r_{ITRF} = \begin{bmatrix} X_{ITRF} & Y_{ITRF} & Z_{ITRF} \end{bmatrix}^{T}$ denotes the position vector in the ITRF (International Terrestrial Reference Frame) [15], where the ITRF is fixed to the Earth and rotates with it. Its origin is at the center of the Earth, its first axis ($\hat{X}_{ITRF}$) extends through the point of latitude 0° and longitude 0°, the second axis ($\hat{Y}_{ITRF}$) is 90° to the east in the equatorial plane, and the third axis ($\hat{Z}_{ITRF}$) extends through the North Pole. $R_{\oplus}$ is the mean equatorial radius of the Earth, $C_{n,m}$ and $S_{n,m}$ are coefficients associated with the tesseral and sectorial harmonics of the Earth, respectively. Also, $P_{n,m}$ is the associated Legendre function of degree n and order m, and the arguments of $P_{n,m}$ are $S_{\lambda} = \sin\lambda$ where λ is the geographic latitude of the satellite, i.e., $S_{\lambda} = \hat{r}_{ITRF} \cdot \hat{Z}_{ITRF}$. Γ_{m} and Π_{m} are defined by the recursion relations:

$$\begin{array}{lll} \Gamma_0 = 1, & \Pi_0 = 0, & (m=0) \\ \Gamma_1 = r_{ITRF}\cdot\hat{X}_{ITRF} & \Pi_1 = r_{ITRF}\cdot\hat{Y}_{ITRF} & (m=1) \\ \vdots & \vdots & \vdots \\ \Gamma_m = \Gamma_1\Gamma_{m-1} - \Pi_1\Pi_{m-1}, & \Pi_m = \Pi_1\Gamma_{m-1} + \Gamma_1\Pi_{m-1}. & (m = 2,3,4,\cdots) \end{array} \tag{44}$$

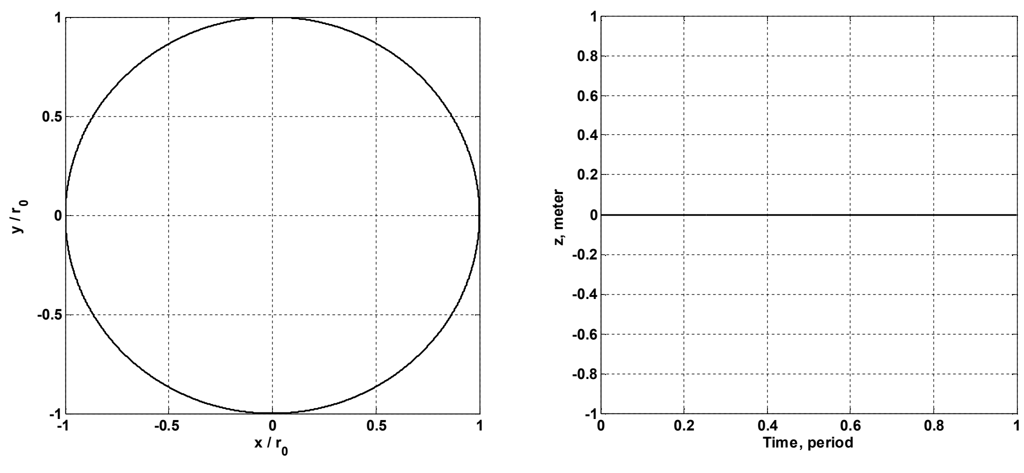

Fig. 1 Controlled trajectory of nominal system using the FECM with no uncertainties

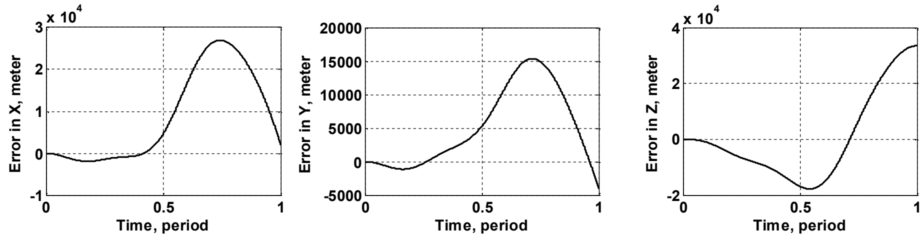

Fig. 2 On-orbit errors of the actual satellite along each axis with $u = 0$

We now assume that the exact nature of this non-spherical gravitational perturbation $\delta\ddot{q}$ given in Eq. (42) that acts on the actual orbiting satellite is not known to us, thereby yielding an uncertainty in our minds with regard to its nature and its description. With knowledge of only an estimate of an upper bound on this uncertain gravitational perturbation $\delta\ddot{q}$, our goal is to make the actual satellite (which is subjected to this gravitational perturbation) track the circular orbit of the nominal system.

Were this uncertainty that is caused by our (assumed) lack of knowledge of this acceleration perturbation to be completely ignored, and only the control, $Q^c(t)$, that was obtained earlier using the FECM with the nominal system employed, the actual satellite's orbit would no longer be circular. Figure 2 shows the resulting errors in the *X*, *Y*, and *Z* directions in the orbit of the actual satellite (in the presence of the gravitational perturbation), where the perturbation model up to the fourth order is assumed, i.e., $n = 4$ is used in Eq. (42). As seen in the figure, the error with $u = 0$ is diverging along each axis.

In order to compare the new PID sliding mode controller developed in this paper with the conventional sliding mode controller given by Eq. (22), the necessary control taking into account the uncertain non-spherical gravitational perturbation is next obtained using the conventional sliding mode controller. The parameters for the controller *u*, are chosen as $b = 1$, $k = 1$, and the upper bound of the uncertainty is set to $\Gamma = 0.05$. This value of the bound is based on the calculation of the infinity-norm of Eq. (42) and depicted in Fig. 3, where $n = 4$ is again used in Eq. (42). It is seen in the figure that the maximum value occurs in the *Z* direction, which is about 0.02 m/s^2.

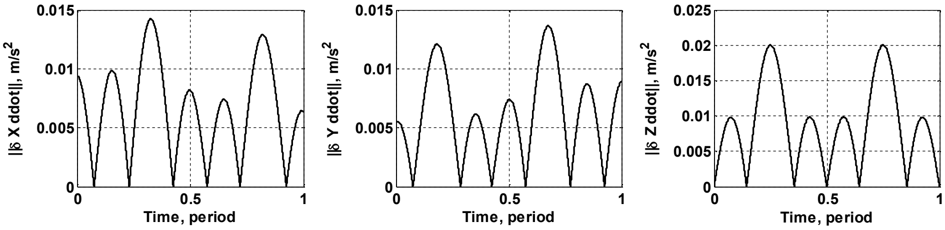

Fig. 3 Infinity-norm of Eq. (42) to calculate Γ

Figure 4 shows the results. The errors along each axis, are bounded and relatively small, compared with Fig. 2. In Fig. 5, the control force along each axis is displayed, showing the chattering problem that arises when conventional sliding mode control is used, i.e., high-frequency oscillations in the control force. This chattering phenomenon is more clearly observed in Fig. 6 in which the control force *u* in the *X* direction is magnified and plotted only for 10 seconds (between 3500 and 3510 seconds, corresponding to between 0.6004 and 0.6022 period). One observes that conventional sliding mode control generates a kind of bang-bang control with the maximum value of *u* in the *X* direction of 0.05 m/s^2. This shows that the last term, $-\Gamma \operatorname{sgn}(s_i)$, in Eq. (22) dominates the control force *u*, and this term is seen to be very sensitive to the value of Γ that is chosen for describing the uncertain (and unknown) gravitational perturbation $\delta\ddot{q}$.

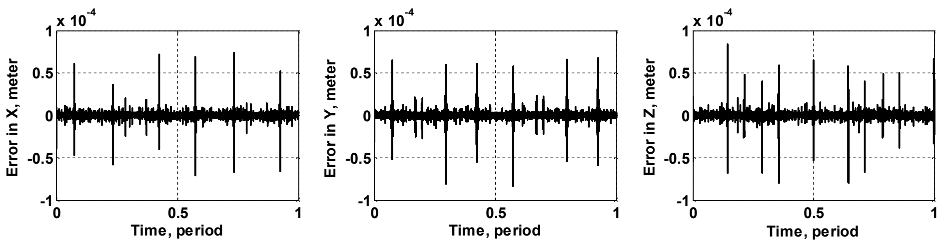

Fig. 4 On-orbit errors of the actual satellite with conventional sliding mode control

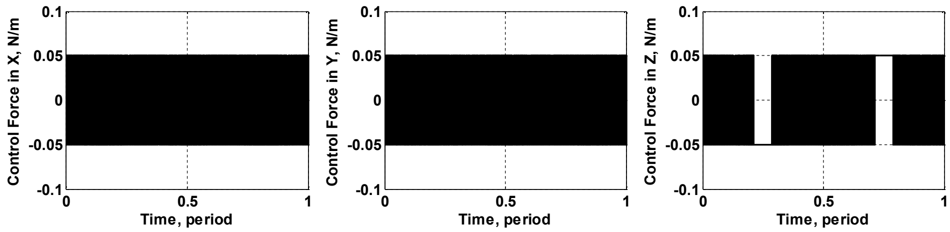

Fig. 5 Control force *u*, along each axis with conventional sliding mode control

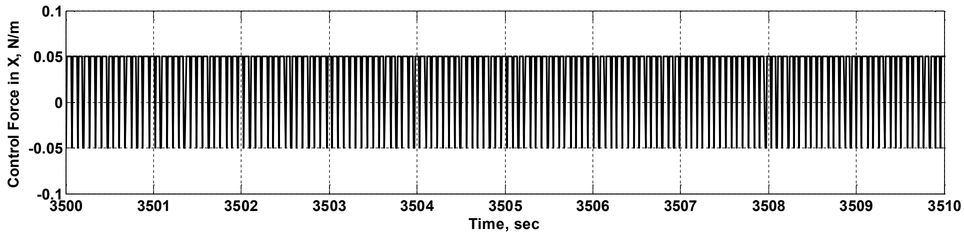

Fig. 6 Chattering phenomenon generated with conventional sliding mode control

For comparison, the new PID sliding mode controller given by Eq. (35) that is proposed in this paper is used for the same problem. We use the parameters, $b=1$, $k=1$, $\varepsilon=0.01$, $\Gamma=0.05$, and $\eta=50$. Figure 7 shows the on-orbit errors of the actual satellite along each direction, and comparing with Fig. 4, one observes that the errors have reduced by about an order of magnitude. In Fig. 8, the control force *u* along each axis is depicted. The magnitude of the control force is again seen to be smaller by about an order of magnitude, compared with Fig. 5, and more importantly, the chattering problem is clearly removed. As illustrated here, the PID sliding mode control is superior to conventional sliding mode control in both tracking accuracy as well as in reducing the magnitude of the control *u* employed.

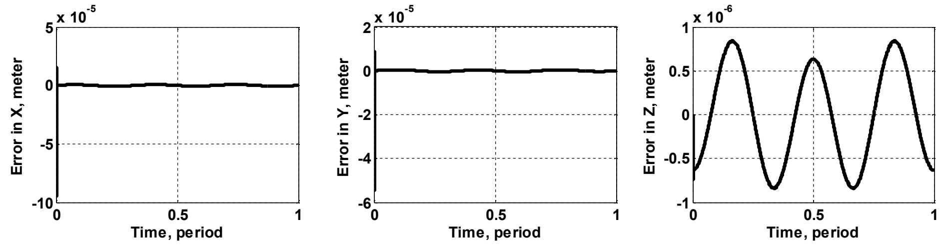

Fig. 7 On-orbit errors of the actual satellite with new PID sliding mode control

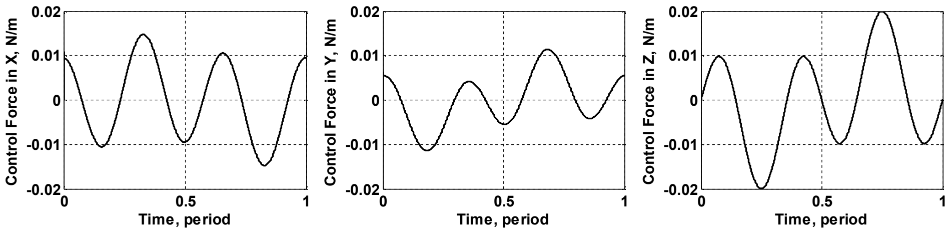

Fig. 8 Control force *u* along each axis with new PID sliding mode control

5 CONCLUSIONS

In this paper a new methodology for the reference-tracking problem is proposed. Two independent control strategies are developed and combined to precisely track the required reference trajectory even under severe uncertainties. The novelty of the proposed approach is that first we readily obtain the explicit form of the exact control force employing the concept of the FECM for the nominal, nonlinear, non-autonomous dynamical system, ensuring that the desired trajectory is exactly tracked while simultaneously minimizing the L_2-norm of the control force at each instant of time. Then, by taking into account uncertainties in the real-world system, a new, continuous sliding mode controller (SMC) is designed so that the chattering problem is alleviated. In addition, numerous forms of the control function are possible depending on practical considerations and a simple special PID-form of SMC is shown to guarantee high robustness while having all the familiar advantages of PID control. By simulating orbital station-keeping under atmospheric drag and uncertainties in the gravitational field, we have illustrated the simplicity and efficacy of the proposed approach which shows great improvement compared with conventional SMC. Future work will include a rigorous investigation of the effects of selecting different functions $f\left(s_i\right)$ on the control performance and the development of an adaptive Lyapunov function flavored with optimality concepts that can be tuned in real time.

REFERENCES

[1] D.E. Kirk, *Optimal control theory: an introduction, 1st Edition*. Dover Publications, 2004.

[2] F.E. Udwadia, Equations of motion for mechanical systems: a unified approach. *International Journal of Non-Linear Mechanics*, **31**, 951-958, 1996.

[3] F.E. Udwadia, A new perspective on the tracking control of nonlinear structural and mechanical systems. *Proceedings of the Royal Society of London, Series A*, **459**, 1783-1800, 2003.

[4] F.E. Udwadia, Optimal tracking control of nonlinear dynamical systems. *Proceedings of the Royal Society of London, Series A*, **464**, 2341-2363, 2008.

[5] H. Cho, A. Yu, New approach to satellite formation-keeping: exact solution to the full nonlinear problem. *Journal of Aerospace Engineering*, **22**, 445-455, 2009.

[6] H. Cho, F.E. Udwadia, Explicit solution to the full nonlinear problem for satellite formation-keeping. *Acta Astronautica*, **67**, 369-387, 2010.

[7] H. Cho, F.E. Udwadia, Explicit control force and torque determination for satellite formation-keeping with attitude requirements. *Journal of Guidance, Control, and Dynamics*, **36**, 589-605, 2013.

[8] V.I. Utkin, Variable structure systems with sliding mode. *IEEE Transactions on Automatic Control*, **22**, 212-222, 1977.

[9] J.-J. Slotine, W. Li, *Applied nonlinear control, 1st Edition*. Prentice Hall, 1991.

[10] J.J. Slotine, S.S. Sastry, Tracking control of nonlinear systems using sliding surfaces with application to robot manipulator. *International Journal of Control*, **38**, 465-492, 1983.

[11] J.A. Burton, A.S. Zinober, Continuous approximation of variable structure control. *International Journal of Systems Science*, **17**, 875-885, 1986.

[12] T. Massey, Y. Shtessel, Continuous traditional and high order sliding modes for satellite formation control. *Journal of Guidance, Control, and Dynamics*, **28**, 826-831, 2005.

[13] F.E. Udwadia, T. Wanichanon, H. Cho, Methodology for satellite formation-keeping in the presence of system uncertainties. *Journal of Guidance, Control, and Dynamics*, **37**, 1611-1624, 2014.

[14] F.E. Udwadia, R.E. Kalaba, *Analytical dynamics: a new approach, 1st Edition*. Cambridge University Press, 2007.

[15] D.A. Vallado, *Fundamentals of astrodynamics and applications, 2nd Edition*. Microcosm, Inc., 2001.

[16] C. Roithmayr, Contributions of spherical harmonics to magnetic and gravitational fields. *NASA/TM–2004–213007*, 2004.